Title
GRAIN BOUNDARY PRECIPITATION IN ALUMINUM ALLOYS: EFFECT OF BOUNDARY STRUCTURE

Author
Gronsky, R.

Publication Date
1979-09-01

LBL-9737
Preprint

Lawrence Berkeley Laboratory
UNIVERSITY OF CALIFORNIA

Materials & Molecular Research Division

Submitted to Metallurgical Transactions

GRAIN BOUNDARY PRECIPITATION IN ALUMINUM ALLOYS:
EFFECT OF BOUNDARY STRUCTURE

R. Gronsky and P. Furrer

September 1979

Prepared for the U.S. Department of Energy under Contract W-7405-ENG-48

DISCLAIMER

Grain Boundary Precipitation in Aluminum Alloys: Effect of Boundary Structure

R. Gronsky and P. Furrer[+]

Materials and Molecular Research Division
Lawrence Berkeley Laboratory
Berkeley, CA 94720

ABSTRACT

A transmission electron microscope study of grain boundary precipitation in Al-Zn and Al-Zn-Mg alloys has been conducted with emphasis on the influence of localized boundary structure. Intrinsic grain boundary defects are found to have a significant effect on the precipitation sequence in that they assist the emerging precipitates in establishing a low energy habit plane relationship with at least one bordering grain. Under more extreme conditions of unavailable habits or unfavorable intrinsic structures, extrinsic defects dominate the precipitation reaction.

[+]Permanent Address: Swiss Aluminum Ltd., Research and Development, CH-8212, Neuhausen, Switzerland

INTRODUCTION

Aluminum-base alloys containing zinc and magnesium are technologically important as medium-to-high-strength materials. Their most useful properties include a marked age-hardening response after mild quenching, good formability, good weldability, and except for high temperature applications, good corrosion resistance. However, these alloys are also know to be highly susceptible to stress corrosion and brittle intergranular fracture following routine heat treatment. Historically, such problems have been associated with microstructural variations at grain boundaries[1] including precipitate-free zones (PFZ) and boundary-nucleated precipitation reactions. There is therefore considerable incentive for understanding these phenomenon in aluminum alloys to the extent that they may be controlled and alloy properties improved.

In the present research program, the particular subject of grain boundary precipitation is under investigation from this point of view. Its principal objective is to characterize active heterogeneous nucleation sites and preferred growth centers at grain boundaries with respect to boundary structure. Establishing this relationship is seen as a precedent to the eventual control of grain boundary reactions.

There have been previous studies in this field which relate grain boundary precipitate density and morphology to grain misorientation,[2-5] to the coincidence site lattice (CSL) model,[6-9] or to the grain boundary plane.[10-12] These studies reveal that there is a dramatic effect of grain boundary structure, although since the correlations are made through some set of parameters which span the boundary region, the specific role of structural details is obscured. This investigation seeks direct evidence of the effects of localized grain boundary structure on precipitation reactions by high resolution techniques of transmission electron microscopy and diffraction.

EXPERIMENTAL PROCEDURE

The Al-Zn-Mg alloy used in this research was chill-cast to form small (~200 x 100 x 30 mm) rolling billets, homogenized at 450°C for 16 hrs. and quenched in water. Final composition was determined by wet chemical analysis to be (in weight per cent) as follows:

Si	Fe	Mg	Zn	Al
<0.005	<0.005	1.75	4.6	(balance)

By subsequent hot and cold rolling with an intermediate anneal (450°C, 1 hr., water quench), the billets were reduced to 0.2 mm thickness, further solution annealed (450°C, 30 mins., water quench) and aged in an oil bath at 150°C for times ranging between 10 and 10^4 minutes. The results reported in this paper were obtained from the samples aged for 150 mins.

A similar treatment was used on an Al-Zn alloy, shown by wet chemical analysis to contain 20.3 wt.% Zn after aging for 30 mins. at 180°C. Sheet specimens of this material were kept refrigerated until thinned for foils.

Foil preparation was carried out in a double jet polisher using a nitric acid-methanol electrolyte at -25° to -30°C. Specimens were examined in either a Philips EM 301 or a Siemens Elmiskop 102, the latter equipped with a high resolution, double tilt-lift goniometer stage. Through controlled specimen tilting, each grain boundary of interest was characterized according to its axis-angle pair[13] following extensive contrast analysis, including weak-beam microscopy[14] of boundary defects. Correlations were made with the size, density and morphology of the boundary-nucleated second phase particles.

EXPERIMENTAL RESULTS

A. Precipitate Morphologies

There was no difficulty achieving copious grain boundary precipitation in the Al-Zn-Mg alloy, as shown in Fig. 1, even after its mild aging treatment. A dense distribution of the η phase $(MgZn_2)$[15] is observed in both the matrix and the boundary plane, separated by a PFZ approximately 250Å wide. The reaction product in fact gives every appearance in this micrograph of a continuous intergranular film having a thickness of approximately 200Å. This is an oversimplified interpretation, however, as revealed in Fig. 2, which shows the same specimen area after a large-angle (∿45°) tilt. Obviously the morphology of the boundary product is not a continuous film but an array of discrete particles with some tendency foralignment along close-packed <111> directions (traces indicated by dashed lines) referred to the upper grain. From the hemispherical cap morphology of the individual particles, it is apparent that nucleation occurred in this (upper) grain; also the boundary plane parallels one of the (001) cube plane surfaces of this grain.

The observation of aligned grain boundary precipitate arrays was common in a large number of specimens, including those of the Al-Zn binary alloy. However the structural origin of this feature was obvious in only a few instances. Fig. 3 demonstrates one case found in the Al-Zn alloy.

The grain boundary in this micrograph is primarily twist (5.9 ± 0.5° about $[\bar{2}00]$) in nature with a small tilt component (2.5 ± 0.3° about [001]. Diffraction contrast analysis indicates that the dislocation network visible in (a) is comprised of lattice dislocations with $\underset{\sim}{b} = \frac{a}{2}[0\bar{1}0]$. Under the diffraction condition in (b) the dislocations are no longer visible, but an assembly of closely-spaced lenticular precipitates are shown with their long dimensions parallel to the dislocation lines. These results demonstrate that the defect structure of the small angle boundary catalyzes the precipitation reaction.

Other typical morphologies for small angle boundaries are shown in Fig. 4, taken from the same specimen which produced Fig. 3 above. The distinct alignment of small particles in (a) is also due to the intrinsic defect structure of the pure tilt (10.1 ± 0.2° about [1$\bar{1}$0]) boundary. It is noted that the boundary plane for both Fig. 3 and Fig. 4 (a) parallels a (220) plane of one of the slightly misoriented contiguous grains. In Fig. 4 (b) however, the boundary plane is parallel to the more closely packed (0$\bar{2}$0) plane of the upper grain with a resultant change in precipitate morphology. In this instance the precipitates are oriented with their long dimension transverse to the dislocations comprising the pure tilt boundary (7.5 ± 0.2° about [1$\bar{1}$0]); i.e., the defect structure has no particular effect on heterogeneous nucleation.

B. Coincidence Site Lattice Effects

With data on the axis/angle pairs of all boundaries surveyed, correlations could be made between the CSL (or O-lattice[16]) model and the nature of the boundary precipitation reactions. An example of a 39° <100> $\Sigma = 5$ CSL is shown in Fig. 5 for the Mg - containing alloy. The most significant difference here is the coarse distribution of larger particles with no tendency to alignment as in Fig. 1. In addition, most of the particles appear to be associated with an extrinsic dislocation[17] (arrowed) intruding into the boundary plane.

By comparison, Figs. 6 and 7, taken from the same specimen as Fig. 5, show the effect of a near-CSL orientation. Both of these boundaries are within 3° of a $\Sigma = 13$, 22° <100> CSL orientation, and both are very nearly parallel to the trace (double arrows) of a {111} plane from one of the neighboring grains. Besides the much higher density of particles at these boundaries, there is also a much more pronounced alignment along <111> traces (arrowed) and less evidence of association with lattice defects (c.f., Fig. 6). No evidence was found however for any direct effect of intrinsic defects in these boundaries.

C. Role of Grain Boundary Defects

Extrinsic dislocations at the boundary plane were frequently found attached to the boundary-nucleated precipitates, even in the case of large angle grain boundaries. As shown in a dark field micrograph of the same ternary alloy specimen (Fig. 8), the arrays of grain boundary precipitates nucleated in the upper grain (out of contrast) do not closely coincide with {111} traces (arrowed) as before, but follow the curvature of the matrix dislocations trapped at the boundary and within the lower grain. The evidence in this case suggests that the dislocations were present at the boundary prior to nucleation and that they served as preferred nucleation sites.

The pair of micrographs in Fig. 9 are successive dark field images of each grain bordering a large grain boundary precipitate in the binary alloy. Note that the precipitate was nucleated in the lower grain and the entrinsic dislocation attached to the precipitate (large white arrow) is visible only when using a reflection from that grain. The remaining defects within the grain boundary (small arrows) are intrinsic dislocations, visible with both reflections, and comprising a network which increases in density at regions of higher boundary curvature (arrowed in (a)) and near the precipitate (arrowed in (b)).

By weak beam imaging of the ternary alloy (Fig. 10), a network of intrinsic defects (open arrow) was observed to pass, in substrate manner, adjacent to the boundary precipitates which have assumed a {111} habit in the lower grain. The extrinsic defects at the boundary, although in contact with the precipitates, did not have the directionality to suggest that they may have served as nucleation sites. In fact, many appeared to wrap around the precipitates (solid arrow), suggesting that their presence in the boundary succeeded, rather than preceded, the nucleation event.

At higher resolution, the nature of the genesis of the grain boundary precipitation reaction is revealed. Fig. 11 is a lattice image, taken under two-beam tilted illumination conditions[18] and shown at low photographic enlargement in (a), higher enlargement in (b). The scale of these prints is indicated by the dashed lines in (b) indicating the 2.3Å spacing of the imaged (111) planes in the Al-Zn alloy. These planes follow the trace outlined by the double arrow in (a), and appear to be the favored habit of the emerging Zn-rich region distinguished by its darker coloration. Note that the open arrow in the figure points to a region of boundary curvature at which a Moiré pattern is seen (labeled M at higher magnification in (b)), which was demonstrated previously[19] to characterize planar matching between the close-packed planes of the matrix and the newly-formed second-phase material.

DISCUSSION

In generalizing the results of this study, it was never observed that precipitation occurred "randomly" at grain boundaries. There were always indications, most often at higher levels of resolution, that some structural discontinuity dominated the nucleation event, or assisted in enhanced growth kinetics. These findings indicate that grain boundaries can no longer be described in toto as heterogeneous nucleation sites; rather they must be recognized for their role in supplying a variety of possible heterogeneities which may, individually or in combination, catalyze a precipitation reaction.

A. Ordered Boundaries

For example, the results on the $\Sigma = 5$ CSL boundary shown in Fig. 5 are anticipated on this model because a highly ordered boundary is less likely to have available intrinsic defects to assist in the precipitation reaction. Likewise, it is no surprise that extrinsic dislocations are frequently in contact with the observed boundary particles, since these offer advantages during both nucleation and growth of the second-phase product as in the case of precipitation within the matrix grains. Similarly, even small deviations from an exact CSL orientation (Figs. 6 and 7) would provide the necessary structural freedom for enhanced nucleation and the ordered arrays of particles in these boundaries attest, if only indirectly, to the presence of some favorable intrinsic structure supporting their growth. The crystallography of these arrays in all instances indicates that the precipitates prefer a habit plane relationship with their parent grain, seeking in most cases the nearest close-packed matrix plane. Such findings relegate to secondary importance the CSL description of the grain boundaries under study, and emphasize the nature of their defect structure in accommodating the new phase.

B. Grain Boundary Defects

Because they can offer fairly large-magnitude compensating strain fields, extrinsic grain boundary defects would be expected to have pronounced effects as nucleation sites. The above results certainly agree with this notion, when such defects are observed. It therefore follows that grain boundary precipitation, in direct analogy to matrix precipitation, can possibly be encouraged by prior deformation. The only concern would be whether or not such defects survive the annealing response prompted by aging.[20]

Of course, even intrinsic grain boundary dislocations should offer some strain energy reduction during nucleation, but the micrographs presented here show that they serve another, more significant, role. Based upon their appearance in Figs. 9 and 10, these dislocations apparently cause the local structural rearrangements necessary to bring about a habit-plane relationship within the boundary plane. The results of the high resolution study (e.g., Fig. 11) confirm that such rearrangements are vital, even at the earliest stages of growth, and even when only one-dimensional matching is achieved. Futhermore this figure indicates that plane matching at precipitate/matrix interfaces may be a likely precedent to a more complete three-dimensional habit-plane matching.

This particular role of intrinsic grain boundary dislocations also explains in part the formation of aligned precipitate arrays at the boundary plane (c.f., Figs. 2, 6, 7, 10). In network form, such defects can induce sufficient disturbance in the boundary plane to create ledges of favorably oriented close-packed planes for subsequent precipitate growth. A direct confirmation of this arrangement is shown in Fig. 10 (open arrow) where the extrinsic grain boundary defects are seen to terminate within the boundary at the intrinsic dislocation array. In fact there is an abrupt change in contrast of the Pendellösung fringes at the boundary where the array terminates, also indicating the presence of a ledge. It is on such ledges that nucleation is shown to be favored

(Fig. 10) and would be expected, since they incorporate candidate close-packed planes of the surrounding matrix.

Given this role of intrinsic defects, an obvious method for suppressing grain boundary precipitation is suggested, viz., decreasing the mobility of such defects within the boundary plane. In the limit of a completely sessile dislocation substructure, only those boundaries occurring in exact habit plane orientations would favor nucleation. The detailed structure and interactions of these intrinsic arrays, which must be known in order to further understand and control their behavior, are currently under investigation.

CONCLUSIONS

The results of this research on two Al alloys suggest that there is a heirarchy of structural influences on grain boundary precipitation reactions.

(1) First in importance for nucleation of grain boundary precipitates is the establishment of a habit-plane relationship with at least one bordering grain. In the trivial case, the grain boundary plane may coincide exactly with the appropriate close-packed planes; however, where this relationship is not realized, intrinsic grain boundary dislocations are actively incorporated in the necessary structural changes for achieving a proper habit.

(2) During atomic rearrangement at the grain boundary, plane matching between the emerging precipitate nucleus and parent grain is a preferred, if only initial, structural configuration.

(3) Extrinsic defects may serve as nucleation sites whenever the boundary plane is very far removed from a habit plane orientation or is structurally deficient in intrinsic defects to assist in achieving a habit locally.

(4) A transition lattice description of those grain boundaries which catalyze precipitation reactions is much less useful than a complete characterization of the non-equilibrium defect structures present at such boundaries. Particularly with reference to the control of grain boundary phenomena in Al alloys, the nature and interactions of intrinsic defect arrays is of utmost importance.

ACKNOWLEDGEMENTS

Financial support for this work was provided by the Division of Materials Sciences, Office of Basic Energy Sciences, U.S. Department of Energy, under contract number W-7405-Eng-48. Additional support from Alusuisse Research and Development (P. Furrer) is also gratefully acknowledged.

REFERENCES

1. G. Thomas and J. Nutting, J. Inst. Met. 88, 81, (1959).
2. S. Toney and H. I. Aaronson, Trans. AIME 221, 909 (1961).
3. D. Turnbull and R. E. Hoffman, Acta. Met. 2, 419 (1954).
4. J. B. Clarke, in High Temperature, High Resolution Metallography, AIME Conf. Proc., Vol. 38, Gordon and Breach, 1965, p. 347.
5. D. Vaughan, Acta Met. 16, 563 (1968).
6. P.N.T. Unwin and R. B. Nicholson, Acta Met. 17, 1379 (1969).
7. J. LeCoze, C. Ranson and C. Goux, C. R. Acad. Sci. Paris C271, 1120 and 1225 (1970).
8. J. LeCoze, M. Biscondi and C. Goux, C. R. Acad. Sci. Paris C274, 129 (1973).
9. D. B. Williams and J. W. Edington, Acta Met. 24, 323 (1976).
10. P. H. Pumphrey, Scripta Met. 7, 1043 (1973).
11. D. Vaughan, Acta Met. 18, 183 (1970).
12. E. P. Butler and P. R. Swann, in Practical Aspects of Electron Microscopy and Microbeam Analysis, B. M. Sigel and D. R. Beaman (eds.), J. Wiley and Sons, Inc. (1975).
13. J. W. Edington, Practical Electron Microscopy in Materials Science, Monograph 2, Macmillan/Philips Technical Library, Eindhoven, 1975, p. 42.
14. D. J. H. Cockayne, I.L.F. Ray and M. J. Whelan, Phil Mag 20, 1265, (1969).
15. C. E. Lyman and J. B. Vander Sande, Met. Trans. 7A, 1211 (1976).
16. W. Bollmann, Crystal Defects and Crystalline Interfaces, Springer-Verlag, N.Y. (1970).

17. R. W. Balluffi, Y. Komen and T. Schober, Surf. Sci. 31, 68 (1972).

18. R. Gronsky, D. R. Clarke and G. Thomas in Electron and Positron Spectroscopies in Materials Science and Engineering, D. Buck (ed.), Academic Press, 1979, p. 275.

19. R. Gronsky and G. Thomas, Scripta Met. 11, 791 (1977).

20. P. H. Pumphrey and H. Gleiter, Phil Mag. 30, 593 (1974).

FIGURE CAPTIONS

Fig. 1 Bright field image of a high angle boundary in the Al-Zn-Mg alloy showing grain boundary product and PFZ. Axis/angle pair describing the boundary is labeled.

Fig. 2 Same image area as in Fig. 1, but after a large-angle (∿45°) specimen tilt. The boundary precipitates are arranged in discrete arrays, with preferred alignment along <111> directions.

Fig. 3 Small-angle boundary in the Al-Zn alloy imaged to reveal (a) the dislocation substructure and (b) the precipitate morphology at the boundary plane.

Fig. 4 Two small-angle boundaries in the Al-Zn alloy showing (a) particle alignment and (b) independent growth of precipitates. The dislocation structure appears to have no catalytic effect when the boundary plane parallels a cuoe plane of the matrix.

Fig. 5 Bright field image of a $\Sigma = 5$ CSL boundary in the Al-Zn-Mg alloy showing coarse distribution of boundary precipitates connected to extrinsic defects.

Fig. 6 Near - CSL boundary (3° from $\Sigma = 13$) in the Al-Zn-Mg alloy (c.f. Fig. 7).

Fig. 7 Near - CSL boundary (3° from $\Sigma = 13$) in the Al-Zn-Mg alloy (c.f. Fig. 6).

Fig. 8 Dark field micrograph of the Al-Zn-Mg alloy showing particle alignment at the boundary plane which contours the curvature of nearby matrix dislocations rather than the arrowed close-packed directions.

Fig. 9 Dark field micrographs of contiguous grains in the Al-Zn alloy. The large arrow locates an extrinsic defect at the face of the boundary precipitate while the smaller arrows show a high density of intrinsic defects at regions of greater boundary curvature.

Fig. 10 Weak beam images of contiguous grains in the Al-Zn-Mg alloy. The large open arrow identifies an intrinsic defect array beneath the boundary precipitates which causes a local change in orientation of the boundary plane.

Fig. 11 Lattice image of the Al-Zn alloy showing a region of solute enrichment at the grain boundary accompanied by a local fluctuation in the boundary plane. The new orientation of the disturbed region (open arrow) is parallel to the close-packed (111) planes of the lower grain.

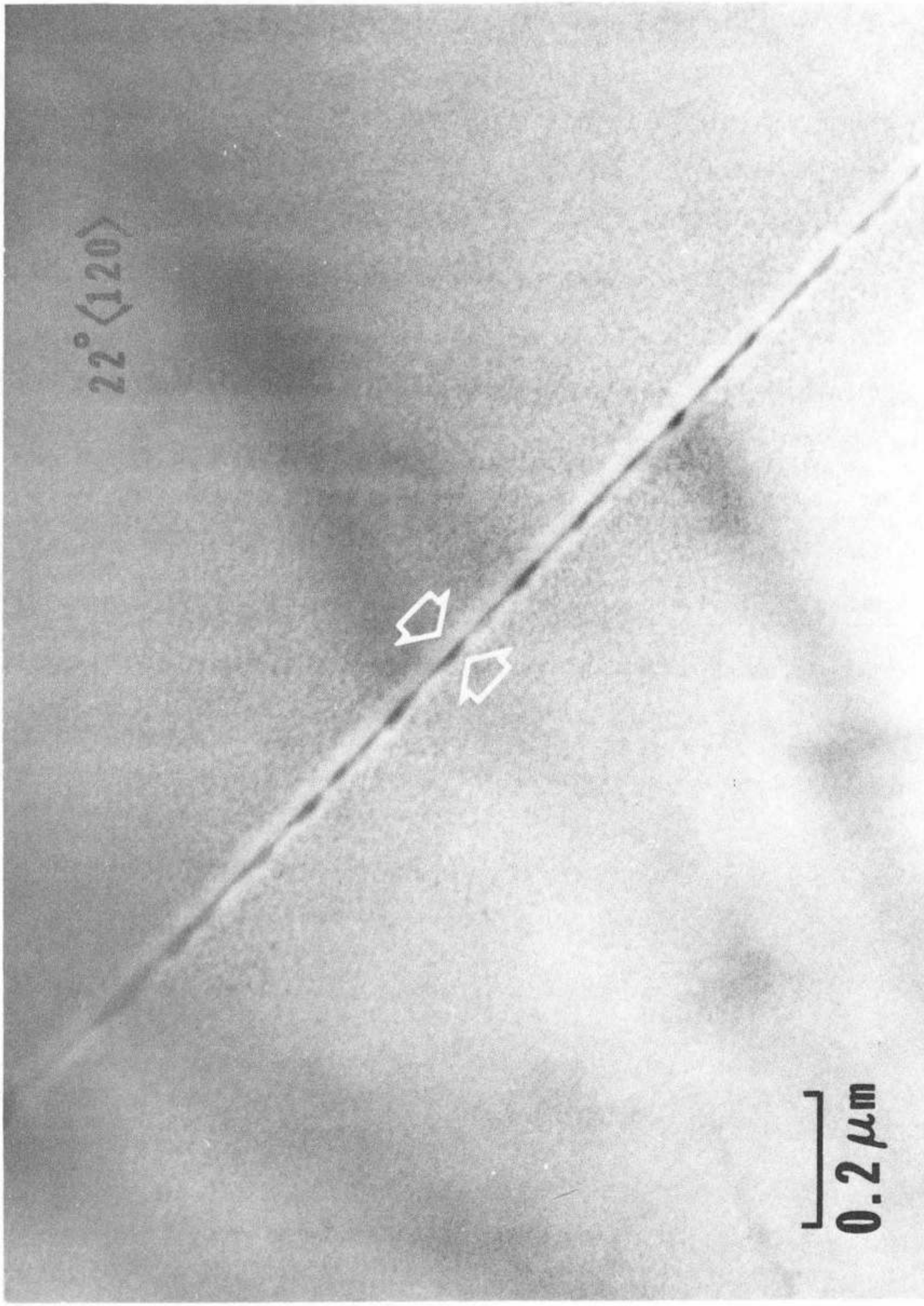

XBB 792-2248

Fig. 1

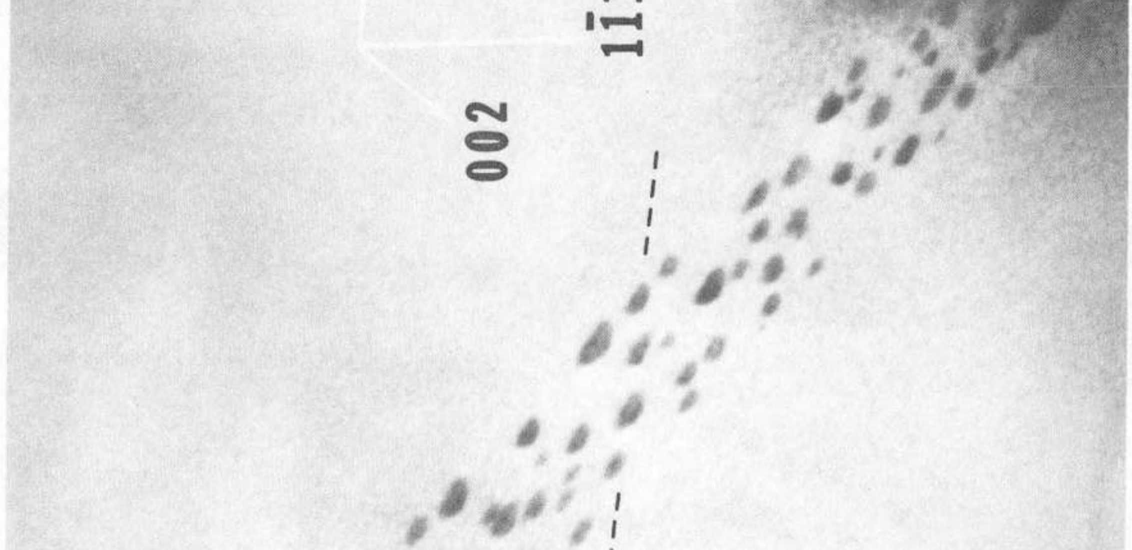

XBB 792-2250

Fig. 2

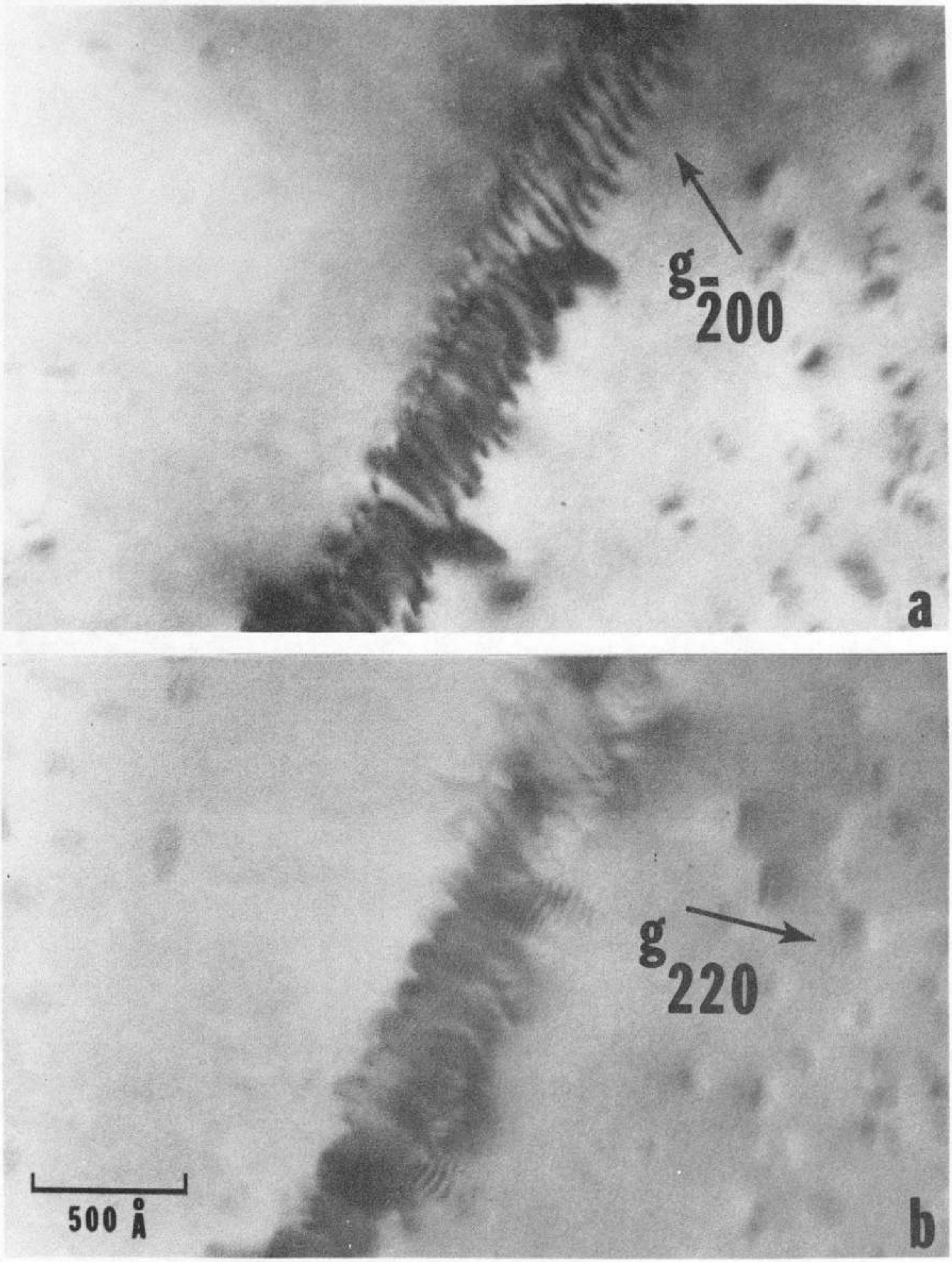

XBB 7611-10518

Fig. 3

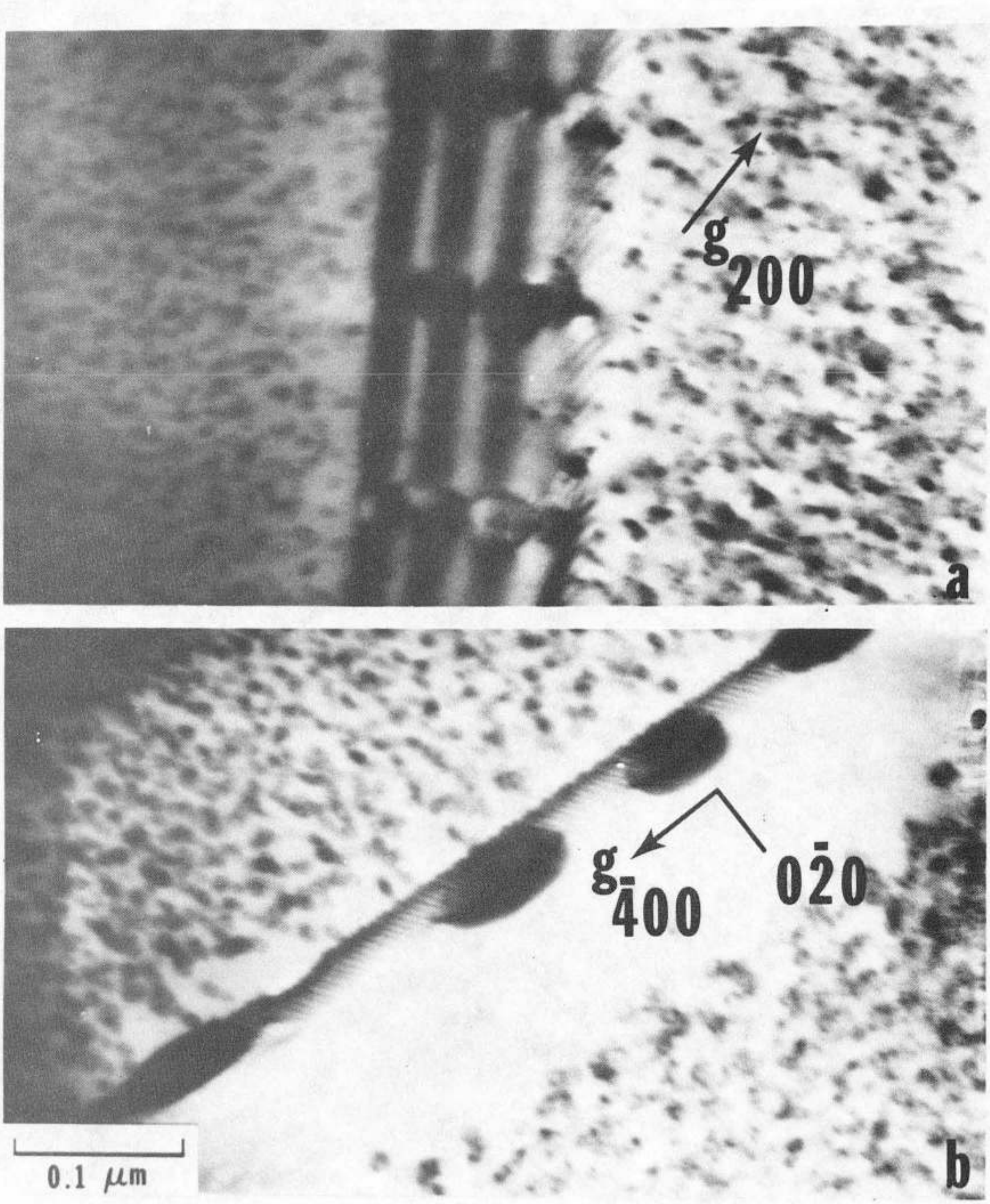

XBB 760-10521

Fig. 4

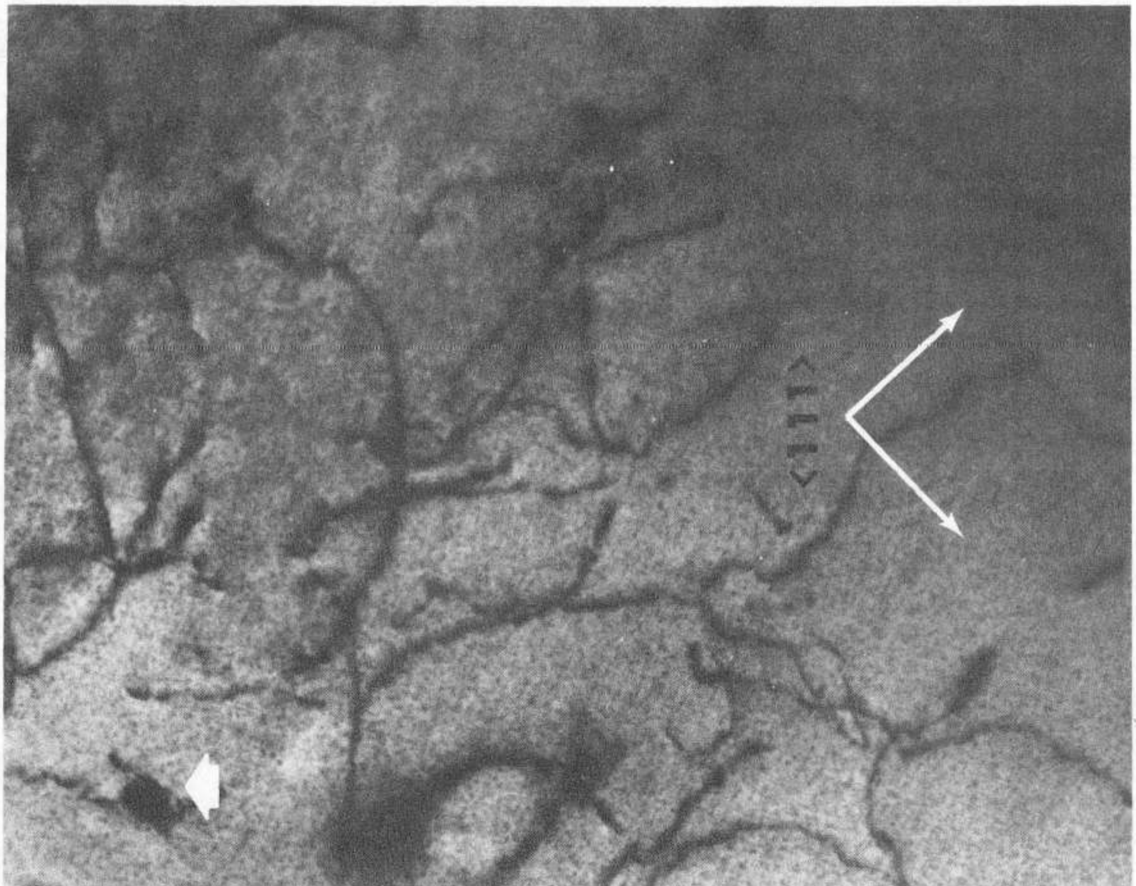

XBB 792-2255

Fig. 5

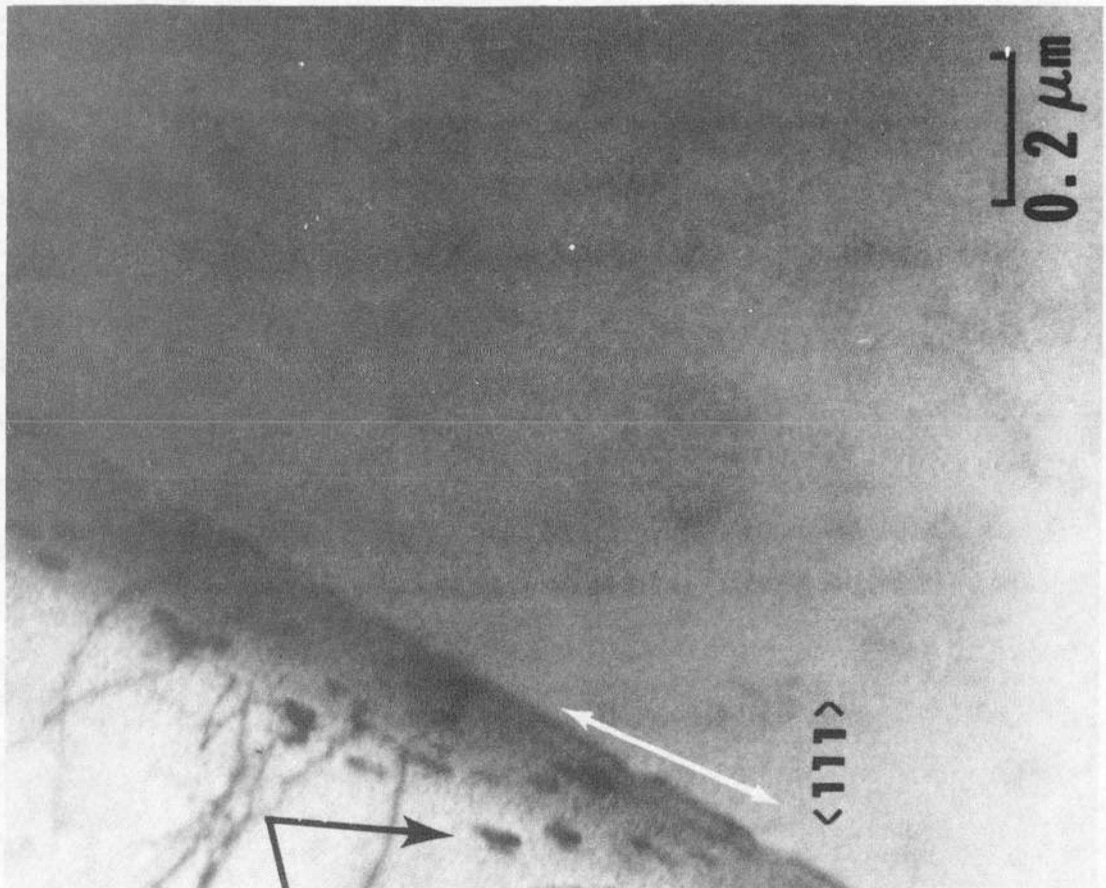

XBB 792-2251

Fig. 6

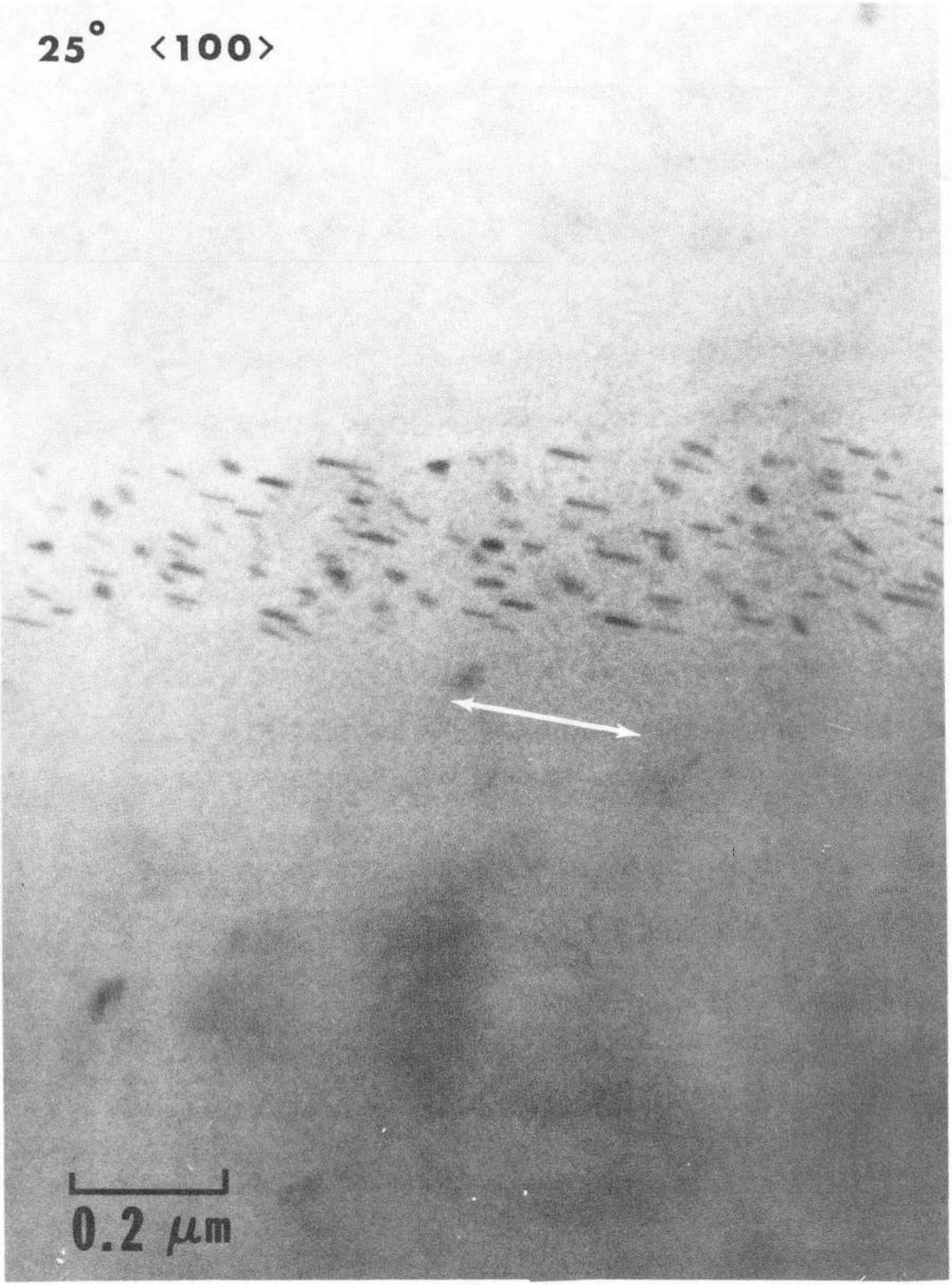

XBB 792-2252

Fig. 7

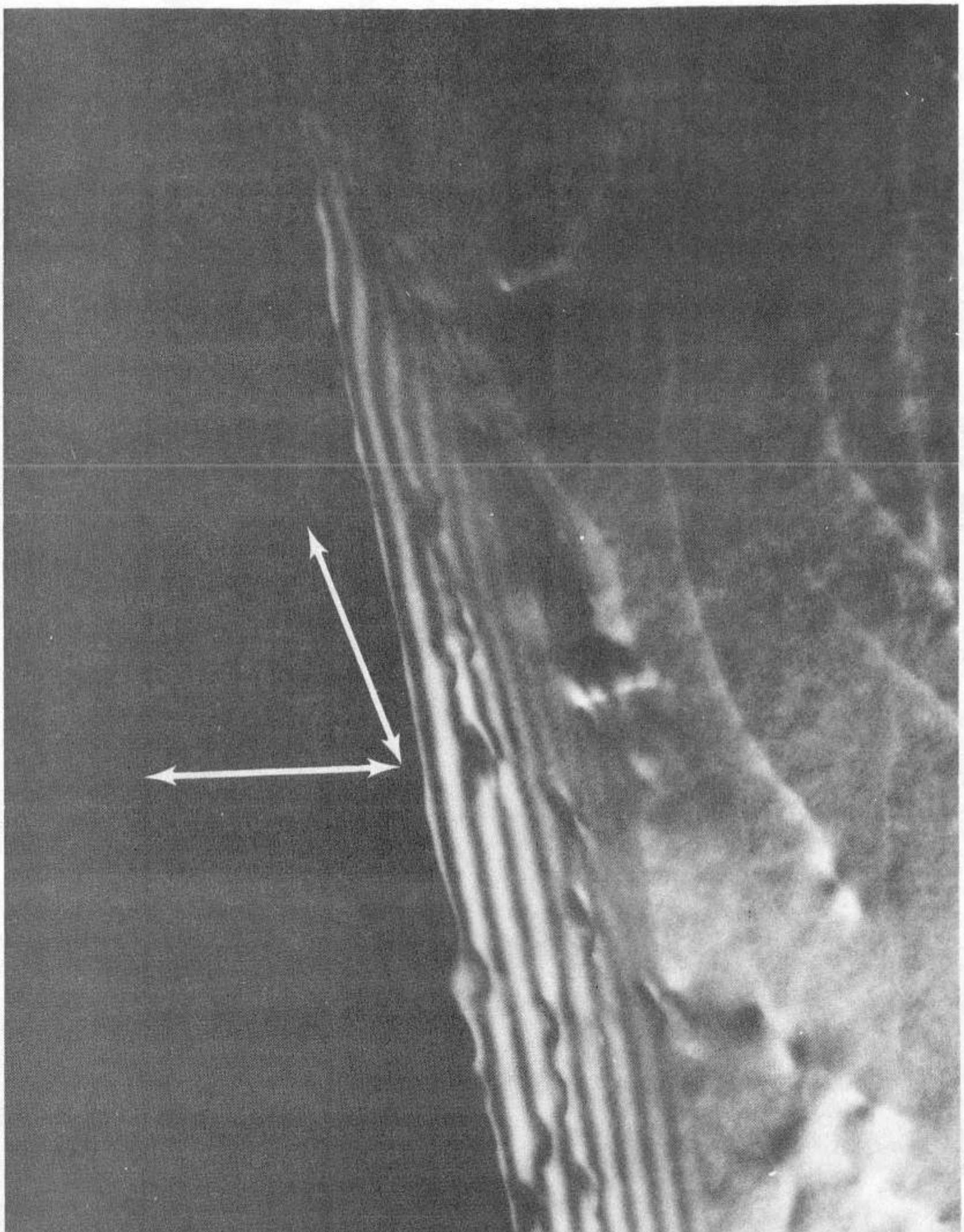

XBB 792-2256

Fig. 8

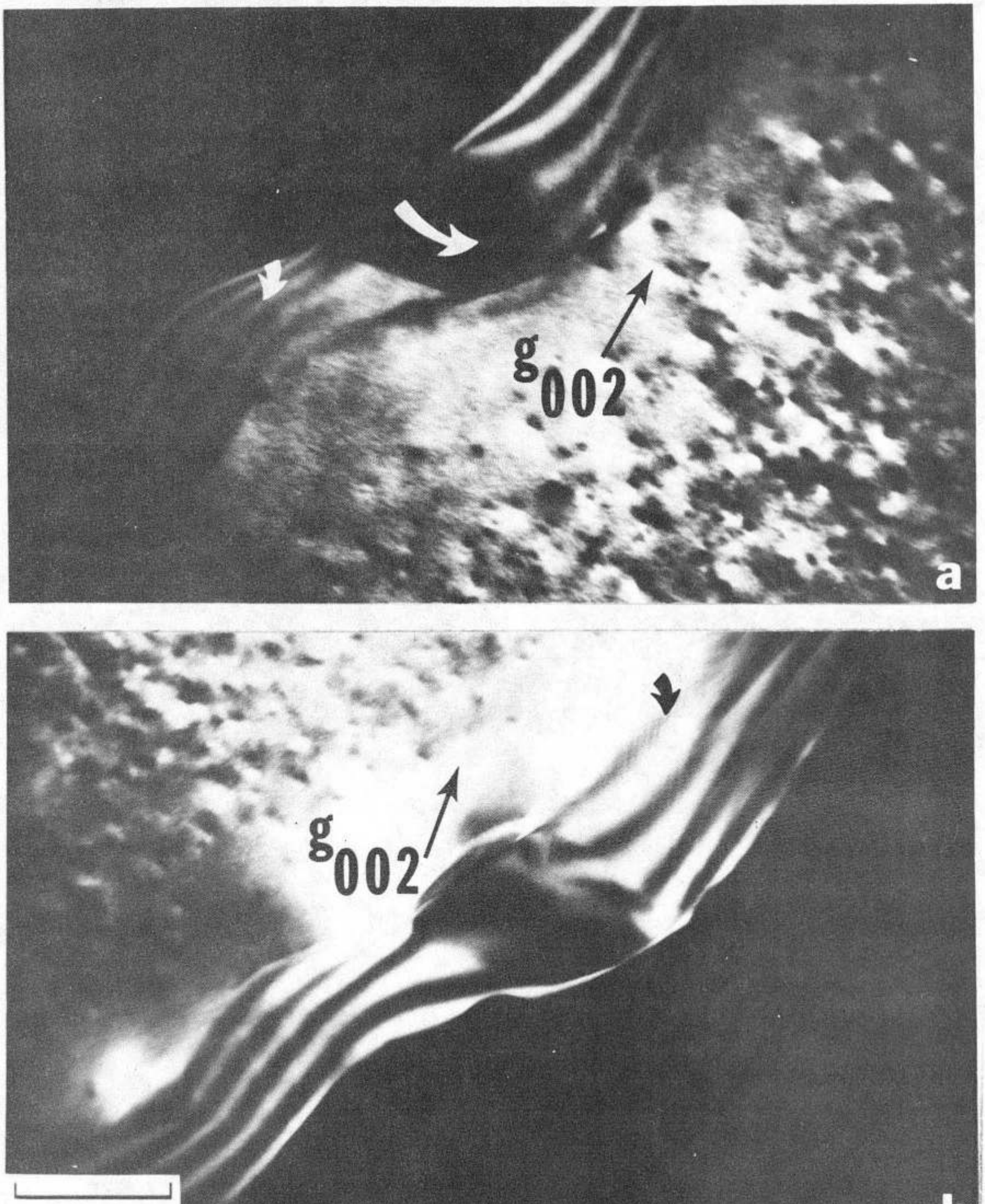

XBB 760-10522

Fig. 9

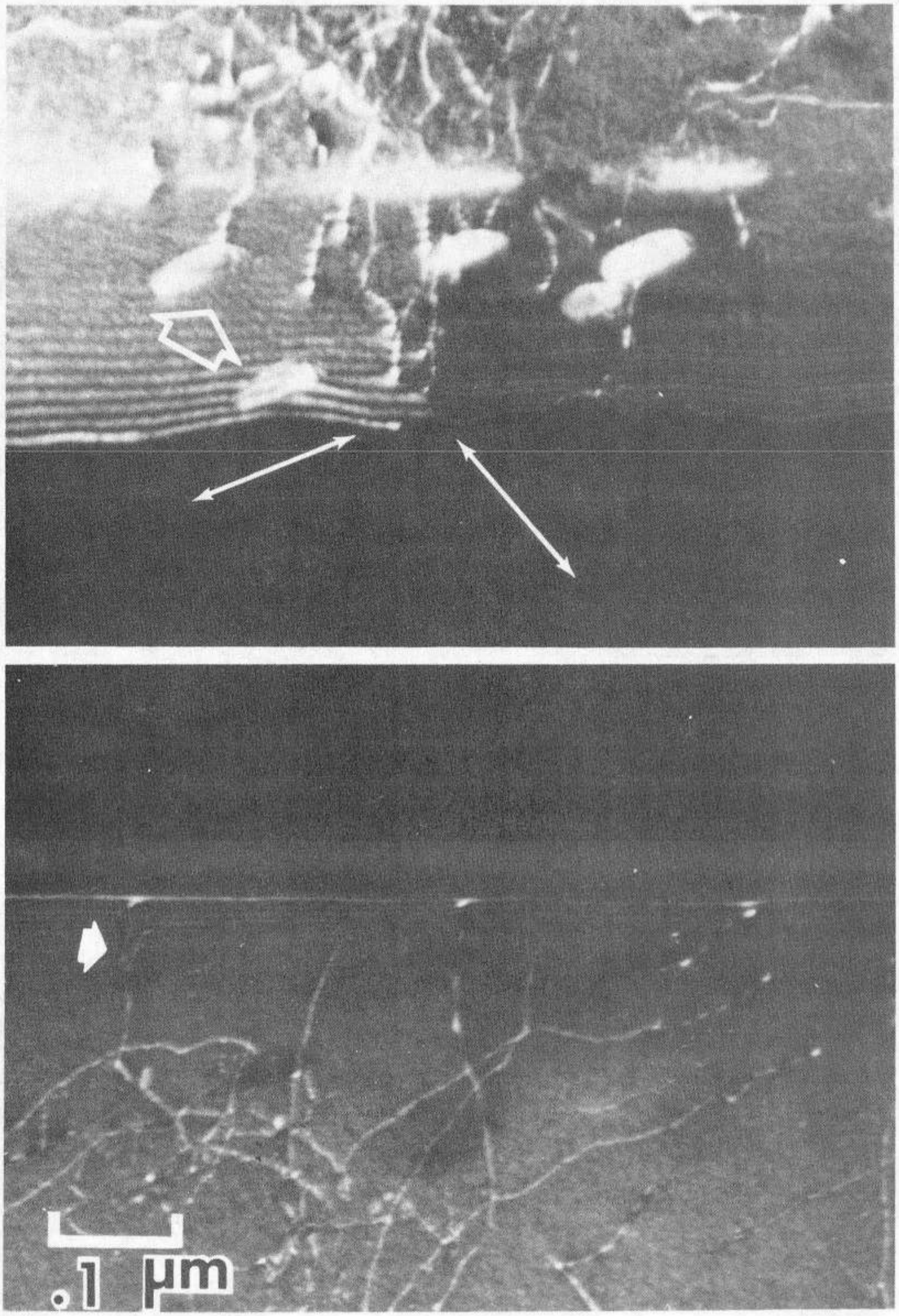

XBB 792-2259

Fig. 10

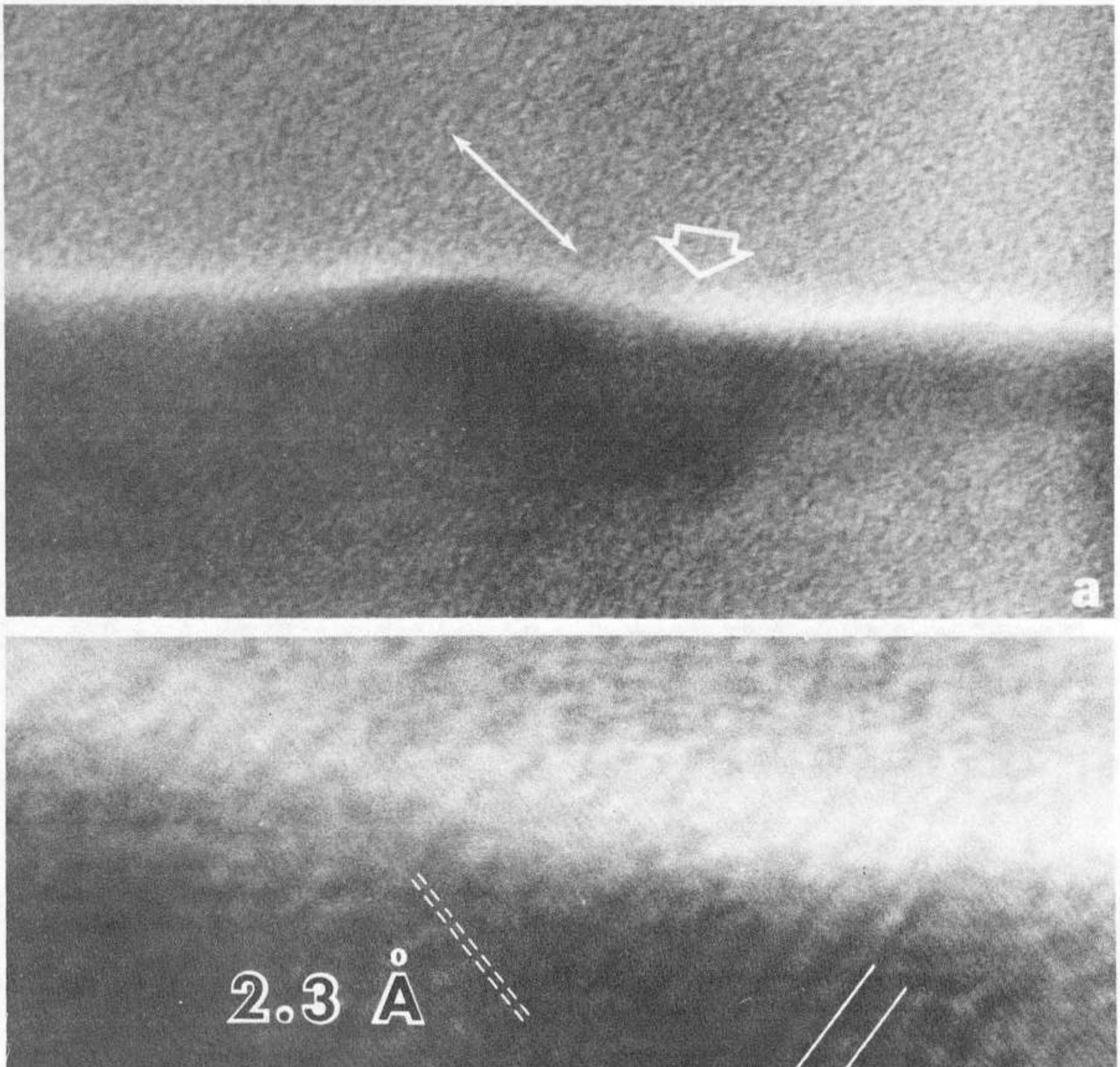

XBB 792-2258

U.S.GPO:1979-689-169 (F) 69

Fig. 11

TECHNICAL INFORMATION DEPARTMENT
LAWRENCE BERKELEY LABORATORY
UNIVERSITY OF CALIFORNIA
BERKELEY, CALIFORNIA 94720